CHEMICAL ENGINEERING TRANSACTIONS
VOL. 81, 2020
A publication of AIDIC
The Italian Association of Chemical Engineering
Online at www.cetjournal.it
Guest Editors: Petar S. Varbanov, Qiuwang Wang, Min Zeng, Panos Seferlis, Ting Ma, Jiří J. Klemeš

ISBN 978-88-95608-79-2; **ISSN** 2283-9216
DOI: 10.3303/CET2081226

Heat Transfer Analysis of a Phase Change Material – Trombe Wall System with the Curtain Structure in Western China

Liqiang Hou, Liu Yang, Tang Liu, Yan Liu*

State Key Laboratory of Green Building in Western China and School of Architecture, Xi'an University of Architecture and Technology, Xi'an, Shaanxi 710055, P.R. China
liuyan@xauat.edu.cn

Trombe wall system is an effective passive solar heating, and phase change material can enhance its heat storage performance significantly. However, excessive heat loss during winter nighttime has been observed. Setting the curtain in air cavity can improve heat preservation of winter nighttime. The three-dimensional model of a phase change material-Trombe wall (TW-PCM) is established with FLUENT, and the influences of phase change temperature (PCT) and location of curtain/aluminum foil on thermal performance of the TW-PCM are obtained. It indicates that the total heat output reduces and the heating time extends for the TW-PCM, and the proportion of glass heat loss is over 50 %. The heat efficiency of the TW-PCM in the nighttime are significantly improved for TW-PCM with the curtain (CTW-PCM). For a TW with an air cavity width of 0.15 m, when the thickness of circulation air cavity exceeds 0.07 m (turbulent flow), heat efficiency is higher. The aluminum foil should attach to the external surface of the curtain.

1. Introduction

According to the World Energy Council, primary energy demand in 2050 will double of that in 2014 (Abbassi et al., 2014). Approximately 30 % of the total world energy is consumed for heating and cooling of buildings (Wang and Li, 2006). Building envelopes thermal performance improvement and renewable energy applications are commonly used to reduce the building energy consumption. A Trombe wall (TW) is an attractive passive solar heating strategy for solar energy utilization in cold and solar rich area (JGJ/T 267-2012). However, thermal comfort at night is difficult to achieve because that large amounts of heat are lost through the glass. Enhancing the preservation of heat at night is crucial for improving the thermal performance of a TW. Two types of insulation comprising insulation outside and inside the cavity are used in TW, where the location of the insulation component differs (JGJ/T 267-2012).

Insulation inside the cavity is a commonly used strategy, where built-in blinds and built-in curtains are the usual methods. Chen et al. (2006) investigated the thermal performance of a TW with a curtain in the air cavity by experiment in Dalian, China. Although the theoretical optimum fixed location for the curtain in the air cavity was obtained to minimize the heat loss, the result was not verified. He et al. (2015) focusing on the base modellig, and after that Hong et al. (2019) considering a specific control application, investigated the thermal performance of a TW with blinds and its impact on the indoor thermal environment in winter. They obtained the optimized design parameters, such as position and tilt angle of the blind and air duct width based on unsteady heat transfer. However, their structures are different from TWs with built-in curtains.

For TWs with built-in curtains, the air cavity is divided into a closed air cavity and a circulated air cavity by the curtain. It has an insulation performance for a closed air cavity. Thermal resistance of the closed air cavity is affected by multiple parameters, such as width of the cavity, emissivity and temperature of cavity surface. Chen (1991) proposed the calculation of air layer thermal resistance, which treated convection and radiation as heat conduction process. Wang et al. (2015) obtained the theoretical additional thermal resistance of a built-in curtain on a glazed window, which took into account the influence of the curtain fold. Qu et al. (2014) investigated the effect of curtain surface emissivity on heat loss on a layer and double layer glass. The function of circulated air cavity is to provide heat to indoor. It is related to flow and heat transfer in the cavity. It is influenced by many factors, such as width of the cavity, emissivity and temperature of cavity surface. For a typical building to avoid

Paper Received: 30/04/2020; Revised: 24/05/2020; Accepted: 17/06/2020
Please cite this article as: Hou L., Yang L., Liu Y., 2020, Heat Transfer Analysis of a Phase Change Material – Trombe Wall System with the Curtain Structure in Western China, Chemical Engineering Transactions, 81, 1351-1356 DOI:10.3303/CET2081226

flow blockage effect, the channel width should be greater than 4.7 cm (Anderson and Kreith, 1987). Gan (1998) studied the effect of cavity width on mass flow rate for a Trombe wall with 0.1 m width inlet, and found that mass flow rate varied within a small range when cavity width is larger than 0.1 m.
However, the optimized structure of TWs with built-in curtain has not been obtained. This is mainly due to the lack of comprehensive analysis of flow and heat transfer in closed and circulated air cavity. In this paper, the complete three-dimensional models of TW-PCMs with built-in curtain are developed with Fluent. The effects of PCT and the location of the curtain/aluminum foil are analyzed. Finally, the optimized structure is obtained for a CTW-PCM.

2. Methodology

2.1 Physical model

A typical CTW-PCM is shown in Figure 1. It is consist of glass cover, closed cavity, curtain, circulation cavity, absorber, PCM, insulation layer and brick layer. In the daytime, the curtain is open and closed in the nighttime. The heated air in circulation cavity rises as a consequence of the buoyancy force and eventually exits from the upper vent, and the cold air is drawn into the cavity through the lower vent. The size of the CTW-PCM is 3.00 m high and 1.00 m width. The distance between the absorber and glass is referred to as the air cavity width, 0.15 m. The curtain divides the air cavity into a closed cavity and a circulation cavity. There are also two air vents (0.40 m width × 0.10 m height) on the massive wall. They are located at 0.10 m away from the top of the massive wall and 0.10 m away from the bottom. The PCM used for analysis is $Na_2SO_4 \cdot 10H_2O$, whose PCT is 32.4 °C–32.5 °C and latent heat is 254 $kJ \cdot kg^{-1}$. Thermophysical properties of materials of the CTW-PCM are listed in Table 1.

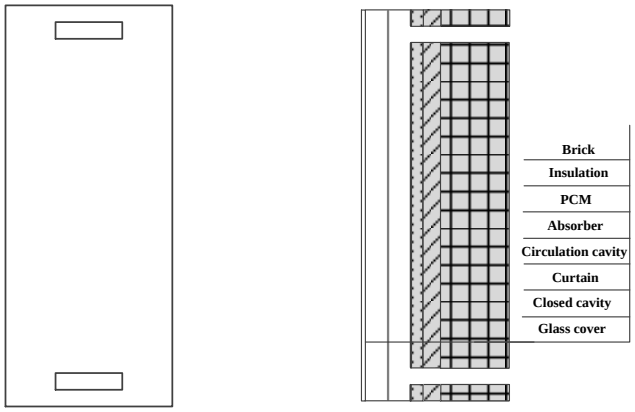

Figure1: Schematic of a three-dimensional typical CTW-PCM

Table 1: Thermophysical properties of materials of the CTW-PCM

Materials	Thickness /m	Density /$kg \cdot m^{-3}$	Thermal conductivity /$W \cdot m^{-1} \cdot °C^{-1}$	Specific heat /$kJ \cdot kg^{-1} \cdot °C^{-1}$
Glass cover	0.005	2,500	0.76	0.837
Curtain	0.003	100	0.045	1.34
PCM	0.020	1,458	0.8	Solid 1.76/Liquid 3.31
Insulation	0.040	50	0.037	1.38
Brick	0.240	1,800	0.814	0.879

2.2 Boundary conditions and solution setup

The weather data of Xi'an typical meteorological year is accessed from Standard for weather data of building energy efficiency (JGJT 3462-2014). And the weather data on January 18 of Xi'an is used for analysis of the CTW-PCMs. The hourly solar radiation of south-facing vertical surface is calculated as Yan and Zhao (1986).
To simplify the mathematical model, the following assumptions and boundary condition setting are made:

(1) The glass external surface is set as the convective boundary, and the convective heat transfer coefficient is fixed as 9.136 $W \cdot m^{-2} \cdot °C^{-1}$ based on the all-day average wind speed of 1.58 $m \cdot s^{-1}$. The hourly outdoor dry-bulb temperature is used as the boundary condition.

(2) The brick internal surface is set as the convective boundary, and the convective heat transfer coefficient is defined as 8.7 $W \cdot m^{-2} \cdot °C^{-1}$. Indoor dry-bulb temperature of 14 °C is used as the boundary condition.
(3) The solar radiant heat absorbed by the glass and massive wall are defined as the heat source by user-defined functions as Yan and Zhao (1986) The absorptivity, reflectivity and transmissivity of the glass and massive wall have been listed in Table 2.
(4) Two air vents are set as pressure boundaries. The inlet temperature is 14 °C, and a temperature of 20 °C as outlet backflow condition.
(5) The perimeters of the glass, PCM, insulation and brick wall are considered as adiabatic.
(6) The cavity air is considered incompressible with constant thermosphysical properties except for the air density, which is treated using the Boussinesq approximation.
(7) The no slip velocity boundary conditions at the surfaces of all layers are assumed.
(8) The PCM is homogeneous isotropic, and property degradation and super-cooling are not considered.

The fully turbulent outer region is modeled using the RNG k-ε turbulence model, and the viscosity-affected near the wall region is completely resolved to the viscous sublayer with Enhanced Wall Treatment for y+<5 (Wolfstein, 1969). The enthalpy-porosity model is adopted for the solidification/melting process of PCMs. The radiation heat transfer of air cavity is calculated using surface to surface (S2S) radiation model. The curtain is open in the daytime and closed in the nighttime. It can be set the air in the daytime and the curtain in the nighttime. The porous media model is used for analyzing the act of the curtain.

The SIMPLE algorithm is employed for the velocity-pressure coupled relations among the governing equations. The up-wind scheme is applied for the convective term.

Table 2: Absorptivity, reflectivity and transmissivity of the glass and massive wall

Materials	Absorptivity α	Reflectivity γ	Transmissivity τ
Glass	0.126	0.074	0.8
Massive wall	0.9	0.1	0.0

3. Grid independence test and model validation

Before the simulation, the grid used in the present study would be checked in the first place. Geometry construction and structured grid with hexahedral elements are developed in the present work. The quality of the grid achieves the best. The outlet air temperature is our focus. The outlet air temperature of a CTW-PCM is chosen to check the grid independence at 19:00. Five grids with different number of elements are employed to check grid independence. The total numbers of grid elements vary from 18,024 to 509,014. The outlet air temperature with 196,557 elements is close to that with 509,014 elements. The grid with 196,557 elements is adopted for the simulation. The grid independence test is shown in Figure 2a and the grid design is shown in Figure 2b.

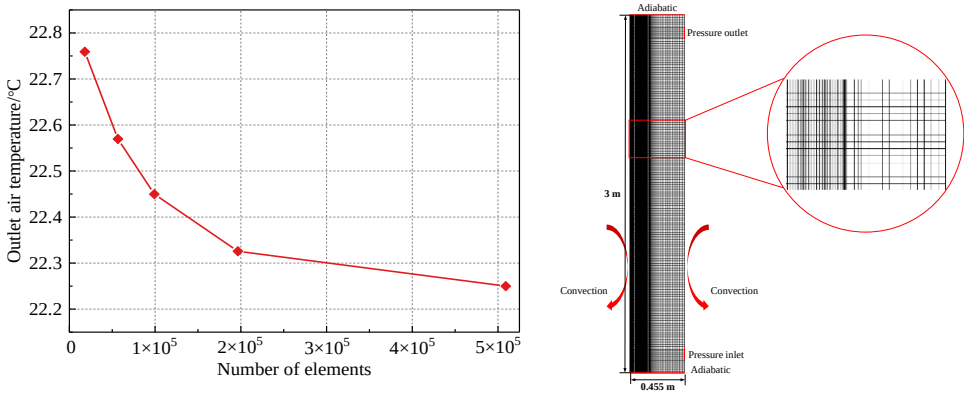

(a) Grid independence test (19:00) (b) Grids of a TW-PCM

Figure 2: Grid data

To test the reliability and accuracy of the numerical model, the simulation results derived from the model are compared with the experimental data. The experiment was carried out in a passive solar house located in Yuzhong city (Gansu Province, China) during March 9–24, 2019. The experiment data of March 15 was used for the comparison. Data were recorded and saved every 10 min. The instruments employed for the tests satisfied ISO Standard 7726-2001. Figure 3 compares the numerical data and experimental test results in terms

of the internal surface temperature of massive wall ($T_{in,\ wall}$), where the results are similar, successfully demonstrating the validity of the model. The mean absolute error (MAE) and root mean squared error (RMSE) were 2.67 °C and 2.74 °C in terms of $T_{in,\ wall}$. The validation demonstrates the reliability of the numerical model for studying the thermal performance of the TWs.

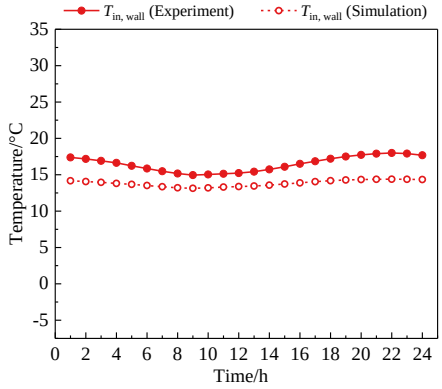

Figure 3: Comparison of numerical and experimental results

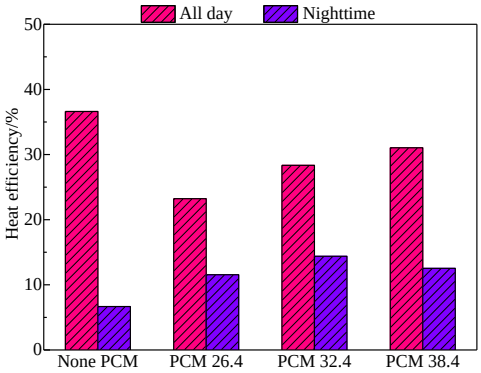

Figure 4: Heat efficiency of Trombe walls

4. Results and discussion

It defines 8:00–17:00 as the daytime and the rest of the time as the nighttime because sunrise at 8:00 and sunset at 17:00 on 18, January in Xi'an.

4.1 The effect of phase change temperature

The PCT has a significant influence on the heat storage of the massive wall. It affects the thermal performance of TWs. The PCTs of 26.4 °C, 32.4 °C and 38.4 °C are analyzed. Heat efficiencies all day of TWs (None PCM, PCM 26.4, PCM 32.4, PCM 38.4) are 36.69 %, 23.20 %, 28.45 % and 30.99 %, and heat efficiencies in the nighttime are 7.84 %, 12.12 %, 14.98 % and 13.51 %, as illustrated in Figure 4. Heat efficiencies all day of TW-PCM decrease, while heat efficiencies in the nighttime increase compared with TW without PCM. In addition, heat efficiencies all day increase as the PCT increases. It is because cavity air temperature is lower than PCT most of the time when PCT is high. And the storage heat of massive wall is less, and most of heat goes into indoor in the daytime.

The heat transfer rate of TWs is showed in Figure 5. It is obvious that the conductive heat transfer rates are less compared with the convective heat transfer rates. It is mainly because the insulation performance of the massive wall is good enough. The heating characteristics vary greatly among different TWs. The total convective heat outputs are 11.26 MJ, 6.43 MJ, 8.29 MJ and 9.22 MJ. Compared with the TW without PCM, the total convective heat outputs are less for a TW-PCM. However, the convective heating time is longer. With the decrease of PCT, the total amount of convective heat transfer decreases and the heating time increases. The uniformity of convective heat output is worse when PCT is higher. That often causes excess and deficiency of heat output.

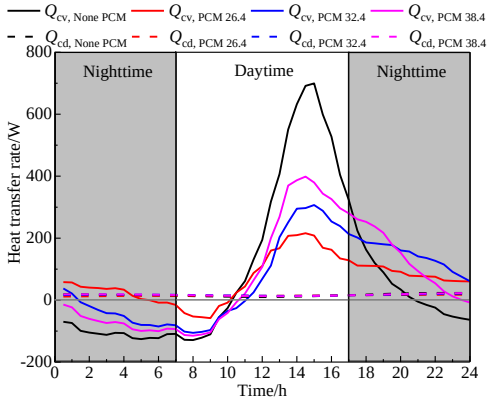

Figure 5: Heat transfer rate of TWs

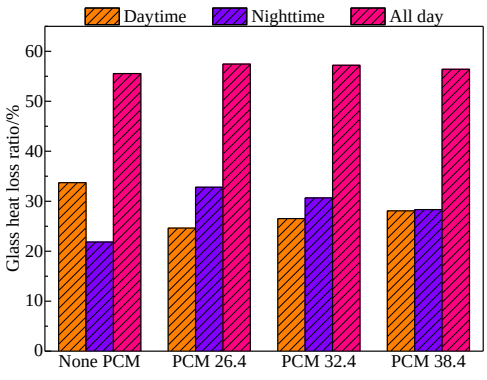

Figure 6: Glass heat loss ratio

The glass heat loss ratios of TWs (None PCM, PCM 26.4, PCM 32.4, PCM 38.4) are 55.54 %, 57.44 %, 57.20 % and 56.40 %, as shown in Figure 6. Glass heat loss ratios in the daytime are 33.71 %, 24.63 %, 26.53 %, 28.07 %, and 21.83 %, 32.83 %, 30.67 % and 28.33 % in the nighttime. Glass heat loss ratio in the daytime will decrease, while that will increase in the nighttime as the PCT decreases. It is notable that the reduction of glass heat loss is of great significance on improving the heat efficiency, especially for glass heat loss in the nighttime. Because glass is merely a heat-loss unit in the nighttime.

4.2 The effect of the location of the curtain

Heat efficiency in the nighttime for CTWs is shown in Figure 7. The thickness of closed cavity of 0.04 m, 0.06 m, 0.08 m, 0.10 m, 0.12 m are analyzed. The total heat efficiencies of CTW-PCMs (No curtain, curtain 0.04, curtain 0.06, curtain 0.08, curtain 0.10, curtain 0.12) are 12.87 %, 20.33 %, 20.48 %, 20.43 %, 16.36 % and 14.76 %, and the convective heat efficiencies are 11.21 %，18.53 %，18.68 %，18.60 %，14.58 % and 12.91 %. The conductive heat efficiencies are less and the differences are small among different CTW-PCMs. The heat efficiency of a TW-PCM in the nighttime is significantly improved when the thickness of closed cavity is less than 0.08 m (the thickness of circulated cavity is larger than 0.07 m). That is because that the air in circulated cavity is turbulent.

Convective heat transfer rate of CTW-PCMs is illustrated in Figure 8. The heat goes into indoor by convection until 1:35, 4:45, 4:40, 4:50, 7:00 and 7:15 for CTW-PCMs (No curtain, curtain 0.04, curtain 0.06, curtain 0.08, curtain 0.10, curtain 0.12), and the total convective heat transfer are 3.64 MJ, 5.99 MJ, 6.04 MJ, 5.76 MJ, 4.71 MJ and 4.17 MJ in the nighttime. The convective heat transfer of CTW-PCMs (curtain 0.04, curtain 0.06, curtain 0.08) increase considerably, compared with TW-PCM without the curtain. It shows that the curtain has a good insulation effect at night. It's interesting that the total convective heat transfer is less, when the heating time is longer. It's obvious that the convective heat transfer change sharply due to the drastic change of air flow, when the curtain is open or closed.

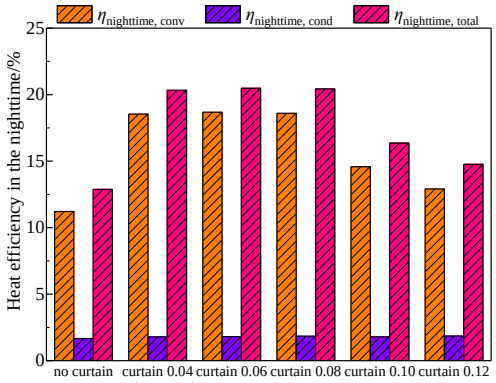

Figure 7: Heat efficiency in the night time

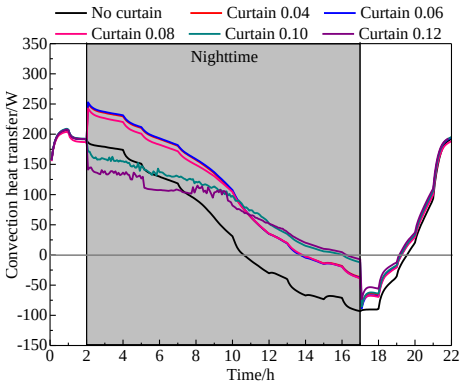

Figure 8: Convective heat transfer rate

4.3 The effect of the location of the aluminum foil

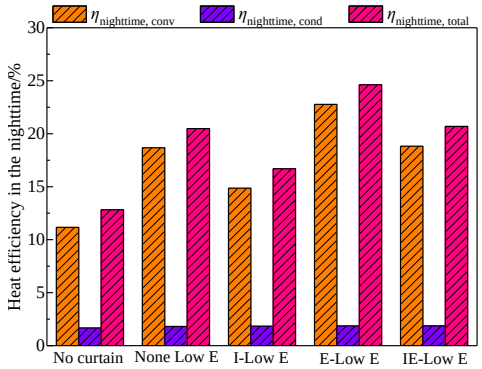

Figure 9: Heat efficiency in the nighttime

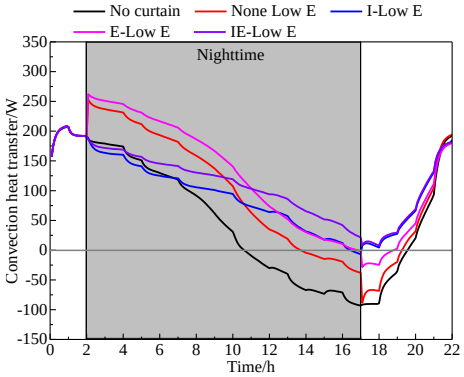

Figure 10: Convective heat transfer rate

Heat efficiency in the nighttime for CTW-PCMs is shown in Figure 9. It's obvious that heat efficiency is the largest for a CTW-PCM which the aluminum foil attaching to external surface of the curtain (E-Low E), and the least for the internal surface (I-Low E). Compared with CTW-PCM (None Low-E), heat efficiency of CTW-PCM (E Low-E) is larger. It indicates the thermal resistance of the closed air cavity has a significant impact on heat efficient. As well, it is unfavorable for attaching to internal surface of the curtain from None Low-E and I Low-E. Due to the combined effect of the aluminum foils of internal and external surfaces, heat efficiency of IE Low-E is slightly higher than None Low-E. In a word, the aluminum foil should be attached to external surface of the curtain.

In order to analyze the cause, convective heat transfer of the circulated air cavity is obtained, as shown in Figure 10. Convective heat transfer of E Low-E increases when the curtain is closed, while decreases for I Low-E. It can inhibit convective heat transfer for attaching to internal surface of the curtain, because of the change of the curtain internal surface and massive wall external surface. As well, the heating time changes.

5. Conclusions

In the present paper, the effects of design parameters on the thermal performance of a CTW-PCM are analyzed based on the numerical simulation. It can conclude that：

(1) Compared with a TW without PCM, the total heat output reduces and the heating time extends for a TW-PCM. The uniformity of convective heat output is better, and heat efficiency in the nighttime increases. Glass heat loss is large, and the proportion is over 50 %. With the PCT decreases, glass heat loss declines in the day and increases at night.

(2) The convective heat transfer and the heating time of a CTW-PCM increase considerably, compared with TW-PCM without the curtain. For a TW with an air cavity width of 0.15 m, when the thickness of circulation air cavity exceeds 0.07 m, heat efficiency is higher. The aluminum foil should attach to the external surface of the curtain.

Acknowledgements

This work was supported by National Natural Science Foundation of China (No. 51838011 and No. 51808429) and Young Elite Scientists Sponsorship Program by CAST, YESS (No. 2018QNRC001).

References

Abbassi F., Dimassi N., Dehmani L., 2014, Energetic study of a Trombe wall system under different Tunisian building configurations, Energy and Buildings, 80, 302–308.

Anderson R., Kreith F., 1987, Natural convection in active and passive solar thermal systems, Advances in Heat Transfer, 18, 1–86.

Chen B., Chen X., Ding Y.H., Jia X., 2006, Shading effects on the winter thermal performance of the Trombe wall air gap: an experimental study in Dalian, Renewable Energy, 31(12), 1961–1971.

Chen Q.G., 1991, Building Thermal Physical Basis, Xi'an Jiaotong University Press, Xi'an, China (in Chinese).

Gan G.H., 1998, A parametric study of Trombe walls for passive cooling of buildings, Energy and Buildings, 27, 37–43.

He W., Hu Z.T., Luo B.Q., Hong X.Q., Sun W., Ji J., 2015, The thermal behavior of Trombe wall system with venetian blind: an experimental and numerical study, Energy and Buildings, 104, 395–404.

Hong X.Q., Leung M.K.H., He W., 2019, Effective use of venetian blind in Trombe wall for solar space conditioning control, Applied Energy, 250, 452–460.

Ministry of Housing and Urban-Rural Development, 2012, Technical Code for Passive Solar Buildings (JGJ/T 267-2012), China Architecture & Building Press, Beijing, China (in Chinese).

Qu J., Song J.R., Qin J., Song Z.N., Zhang W.D., Shi Y.X., Zhang T., Zhang H.Q., Zhang R.P., He Z.Y., Xue X., 2014, Transparent thermal insulation coatings for energy efficient glass windows and curtain walls, Energy and Buildings, 77, 1–10.

Wang D.J., Liu Y.F., Wang Y.Y., Zhang Q., Liu J.P., 2015, Theoretical and experimental research on the additional thermal resistance of a built-in curtain on a glazed window, Energy and Buildings, 88, 68–77.

Wang L.P., Li A.G., 2006, A numerical study of trombe Wall for enhancing stack ventilation in building, The 23rd Conference on Passive and Low Energy Architecture, Geneva, Switzerland.

Wolfstein M., 1969, The velocity and temperature distribution of one-dimensional flow with turbulence augmentation and pressure gradient, International Journal of Heat and Mass Transfer, 12, 301–318.

Yan Q.S., Zhao Q.Z., 1986, Building thermal process, China Architecture & Building Press, Beijing, China (in Chinese).